Development of Gravity Field Calibrator for KAGRA

Rishabh Bajpai[a],* **on behalf of the KAGRA collaboration**

[a]*National Astronomical Observatory of Japan,*
2-21-1 Ōsawa, Mitaka, Tokyo, Japan

E-mail: rishabh.bajpai@nao.ac.jp

The output of a gravitational wave telescope is a voltage signal which needs to be calibrated to get the strain signal h(t). This signal h(t) can then be used to derive various parameters of the gravitational wave sources. Any uncertainty in the calibration is directly transferred to these parameters. Therefore, absolute calibration of gravitation wave detectors using a precise reference (known) signal is essential.

Currently, KAGRA uses Photon Calibrator (PCAL) to generate reference signals for calibration. PCAL injects a power-modulated laser onto the test mass to calibrate the absolute displacement of the mirror using radiation pressure. Hence, the absolute calibration of KAGRA is limited to 3% by the absolute laser power measurement uncertainty due to the deviation in the laser power standards.

KAGRA proposed a new method combining PCAL with Gravity Field Calibrator (GCAL) to reduce the calibration uncertainty. GCAL modulates the test mass using a dynamic gravitational field generated by rotating multipole masses. Since the injected force by GCAL depends on the gravitational constant, mass, distance, rotation frequency, and radius, calibration uncertainty in the sub-percent region can be achieved.

In this paper, we will report on the progress of the development of the gravity field calibrator and our future plans.

*Speaker

1. Introduction

On 14 September 2015, almost 100 years after Einstein's prediction, LIGO Hanford and Livingston made the first direct detection of gravitational waves (GW150914) [1]. Since then, several more events [2–4] have been detected by Advanced LIGO [5] and Advanced Virgo [6], accelerating the field of GW astronomy and providing us with a new way to probe the universe. The current second-generation gravitational waves telescope are ultra-sensitive Fabry-Perot Michelson interferometer with dual power recycling cavities. An incoming gravitational wave stretches one arm of the detector while simultaneously squeezing the other. The interfrometer measures this differential arm-length change at the output port. A gravitational wave telescope's output is a voltage signal that needs to be calibrated to get the strain signal *h(t)*. This signal *h(t)* can then be used to derive the parameters, such as the luminosity distance, masses, spins and sky location of the gravitational wave source binary system. Any uncertainty in the calibration is directly transferred to these parameters. Therefore, the detector must be calibrated using a precise reference (known) signal.

Large-scale Cryogenic Gravitational wave Telescope (KAGRA) [7] is a 3 km arm-length, second-generation gravitational wave detector in Kamioka mine, Gifu, Japan. Currently, KAGRA uses Photon Calibrator (PCAL) [8] to generate the reference signal for the interferometer calibration. Currently, the calibration uncertainty of KAGRA PCAL is around 3% [9, 10]; thus, a new calibration method is required. One candidate for reducing calibration uncertainty is a gravity field calibrator. It modulates the test mass using a gravity gradient generated by rotating multipole masses and can achieve calibration uncertainty in the sub-percent region. In this paper, we report the current status and future plans for GCAL development.

2. Photon Calibrator

The schematic of Photon calibrator (PCAL) is shown in fig. 1. PCAL injects a power-modulated laser onto the test mass. The radiation pressure from the power modulated laser imparts a known force (displacement) to the test mass. The displacement of the test mass (x) can be described as;

$$x = \frac{P\cos(\theta)}{2c} s(\omega) \left[1 + \frac{M}{I}\vec{a} \cdot \vec{b}\right] \quad (1)$$

where P is the absolute laser power, θ is the incident angle of the PCAL laser, c is the speed of light, ω is the angular frequency, $s(\omega)$ is the force to displacement transfer function (approximated as $\frac{1}{M\omega^2}$ above 20 Hz), M is mass of the test mass, $\vec{a}$ and $\vec{b}$ are position vector of the PCAL and main laser beams and $I = \frac{Mh^2}{12} + \frac{Mr^2}{4}$ is the moment of inertia, where h and r are height and radius of the mirror.

The force imparted by the PCAL can be derived by measuring the injected laser power. The laser power is monitored by integration spheres at the transmitter (V_{TxPD}) and receiver module (V_{RxPD}). Therefore, the absolute calibration of KAGRA is limited by the absolute laser power measurement uncertainty due to the deviation in the laser power standards. Comparison of absolute laser power standards between several countries has shown the systematic error of larger than 3%. KAGRA proposed a promising solution to reduce calibration uncertainty in the Photon Calibrator
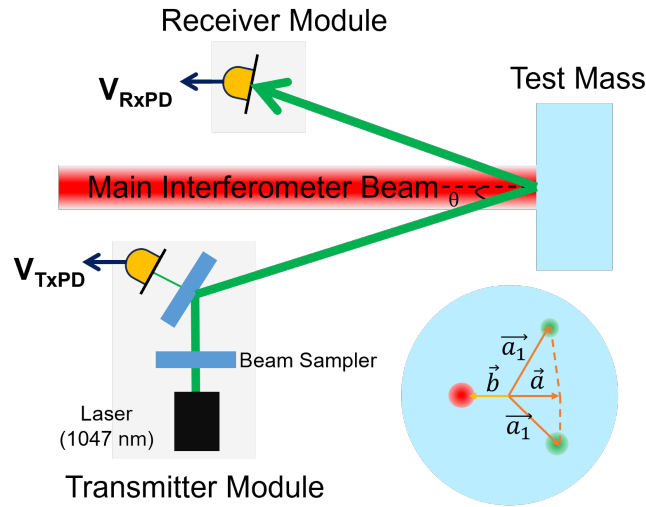
Figure 1: Schematic of Photon Calibrator from [11]. The laser is housed inside the transmitter module. The laser power P is monitored at the transmitter and receiver module. KAGRA PCAL is third-generation PCAL where two input beams injected to actuate the test-mass. Note that beam position are exaggerated to highlight vector $\vec{a}$ and $\vec{b}$.

in [11]. The idea is to combine the current PCAL with a Gravity Field Calibrator (GCAL) to reduce the absolute calibration uncertainty. In next the section, the principle of gravity field calibrator is described.

3. Gravity Field Calibrator

The GCAL modulates the test mass using a dynamic gravitational field generated by rotating multipole masses, as shown in fig. 2a. The rotor with the multipole masses is housed in a vacuum to minimize acoustic noise coupling. The multipole is defined as the number of masses, N on the

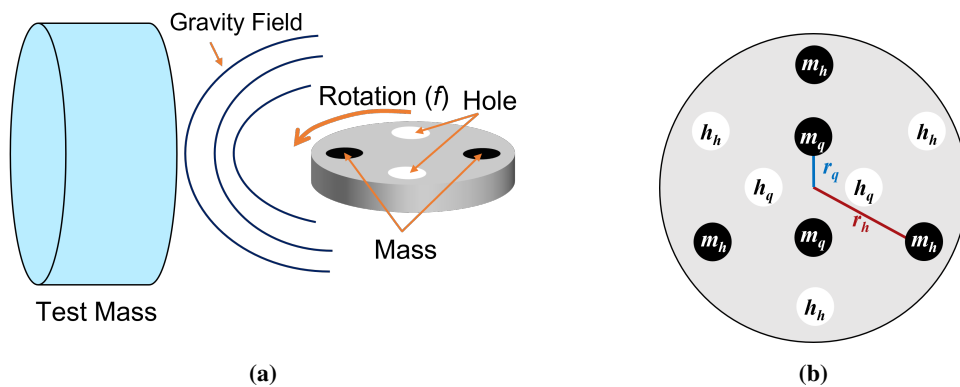(a)   (b)

Figure 2: (a) A simple schematic illustrating the principle of Gravity field calibrator. (b) The rotor of GCAL showing the qudrupole and hexapole mass distribution. For a rotor frequency f the test mass is modulated at $2f$ and $3f$ by quadrupole and hexapole, respectively. The subscript q and h indicate quadrupole and hexapole, respectively and m and h indicate mass and hole, respectively.
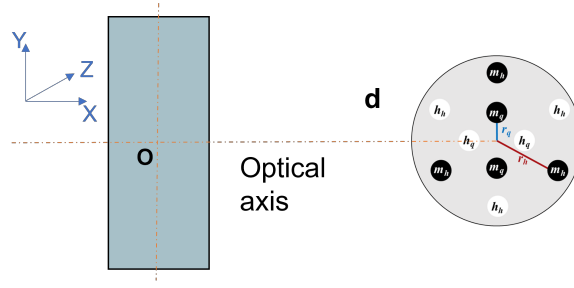
Figure 3: Schematic top view of gravity field calibrator. The center of test mass is fixed as origin in this reference frame. The rotor is placed at a distance *d* along the optical axis.

rotor. As shown in fig. 2b, the rotor consists of a quadrupole ($N = 2$) (made of 2 masses m_q and 2 holes h_q) and a hexapole ($N = 3$) (made of 3 masses m_h and 3 holes h_q) mass distribution. When a motor rotates the rotor at some frequency f, the test mass is modulated at $2f$ and $3f$ by quadrupole and hexapole, respectively.

Figure 3, shows the schematic view of the gravity field calibrator with the test mass at the origin. The rotor is placed in the XY plane with $Z = 0$ at a distance d along the optical axis. Assuming all the masses in the GCAL-TM system as point masses, the displacement of the TM can be derived using Legendre polynomial, as shown in [11].

The magnitude of test-mass displacement due to quadrupole, x_{2f} is

$$x_{2f} = 9\frac{GMm_q r_q^2}{d^4}s(\omega) \tag{2}$$

And, the magnitude due to hexapole, x_{3f} is

$$x_{3f} = 15\frac{GMm_h r_h^3}{d^5}s(\omega) \tag{3}$$

In eqs. (2) and (3), G is the gravitational constant, M is TM mass, m_q is mass of each quadrupole cylinder, m_h is mass of each hexapole cylinder, r_q is the radius of the quadrupole, r_h is the radius of the hexapole, d is the distance between rotor, and TM and $s(\omega)$ is the force to displacement transfer function. Since the injected force on the test mass depends on the gravitational constant, mass, distance, frequency and radius, calibration uncertainty in the sub-per cent region can be achieved. The dominant uncertainty contribution is the measurement precision of rotor-mirror distance.

4. Current Status

4.1 Design and Development

Figure 4a shows the schematic of KAGRA GCAL. The GCAL at the KAGRA site will be placed 2900 *mm* from the test mass at an angle of 40° from the optical axis on a stainless steel pylon. The design values of each parameter of GCAL and their uncertainty are summarized in table 1. The rotor is made from aluminum while the masses are cylinders made from tungsten. A commercial speed control motor, *Oriental SCM590JA-2*, drives the rotor. The maximum speed of this motor is 1600 *rev/min*, which is down-converted by a gearbox to 800 *rev/min*. This means the
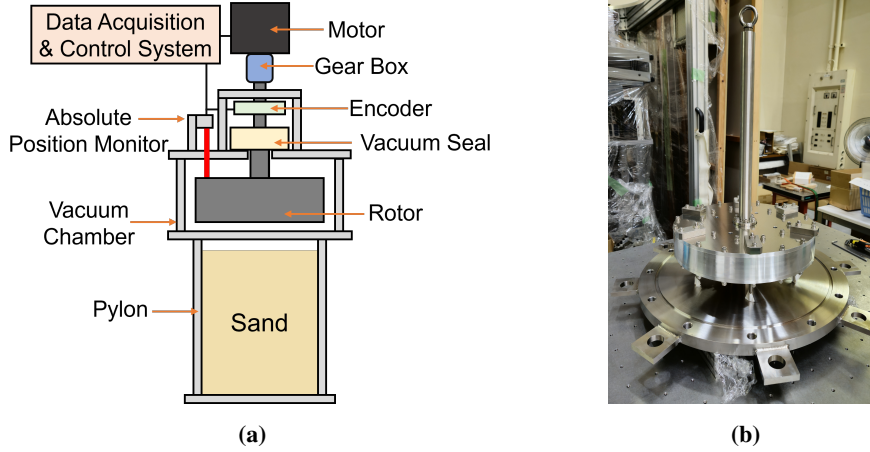
(a)
(b)

Figure 4: (a) Schematic of gravity field calibrator indicating the various components. (b) Photo of partly assembled GCAL showing the rotor and base of the vacuum chamber.

Table 1: Parameters of KAGRA GCAL and their uncertainties (in mm). These values were used for the numerical model in section 4.2. The comment row shows what the uncertainty indicates.

Parameter	Tungsten Mass		Radius of multipole mass distribution		Rotor-TM Distance		
	Height	**Radius**	**4-pole**	**6-pole**	**X**	**Y**	**Z**
Design Value	50	50	80	135	2221.577	1864.121	0
Uncertainity	0.01	0.01	0.002	0.004	3	3	3
Comment	Precision of measurement		Standard deviation of measured radii on the rotor		Expected precision of survey		

max $2f$ and $3f$ frequencies are $\approx 27Hz \approx 40Hz$, respectively. The design of the absolute position monitor and DAQ system is still ongoing. The individual components have been procured, and we are currently assembling the prototype GCAL as shown in fig. 4b.

4.2 Numerical Model

From eqs. (2) and (3), we can approximate the order of force induced by the GCAL. However, a detailed numerical model is required to calculate the precise magnitude and uncertainty of the injected force. This is because eqs. (2) and (3) approximate all the masses as point masses. Furthermore, fig. 3 shows a simple model of the GCAL, and in reality, GCAL will be placed at some angle from the optical axis since the vacuum duct runs along the optical axis.

The numerical model is developed using finite element analysis software Ansys and is built on a previous model used to evaluate Newtonian noise from the KAGRA cooling system [12]. The model breaks down the test mass and tungsten masses into a finite-element mesh, as shown in fig. 5. The force is then calculated as the sum of all forces between each pair of elements, one in the "rotor" mesh and the other in the "test mass" mesh (using a code written in Ansys Parametric
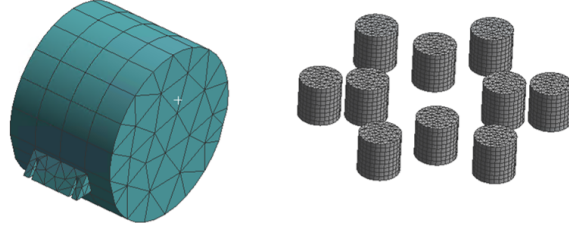
Figure 5: Screenshot of the meshed GCAL model showing KAGRA sapphire test mass with ears and tungsten masses for the quadrupole and hexapole distribution.

Table 2: Force due to quadrupole and hexapole calculated using the point-mass approximation and Ansys model. For this calculation, the density of TM (sapphire) and tungsten masses was assumed to be constant. Furthermore, it is assumed that the height and radius of each tungsten mass in a particular iteration are the same. The force was calculated for 8 rotor position, ($\omega_r t = 0°, 60°, 90°, 120°, 180°, 240°, 300°, 360°$). For each rotor position 800 iterations were performed. Results of the 8 rotor positions for each iteration were fitted to calculate the force magnitude. The mean and standard deviation of the magnitude calculated from 800 fittings are considered as calculated value and uncertainty. A detailed simulation with measured dimensions and uncertainty will be performed next.

Multipole	Force [pN]			
	Point-Mass Approximation		**Finite Element Model**	
	Magnitude	**Uncertainity**	**Magnitude**	**Uncertainity**
Quadrupole	2.328	0.005	2.044	0.005
Hexapole	0.51	0.001	0.466	0.001

Design Language). The force due to a mass/hole on the test mass along the optical axis (X) at particular rotor position ($\omega_r t = [0°, 360°]$), $F_{m/h}$ is:

$$F_{m/h} = G\rho_{tm}\rho_{m/h} \sum_{g=1}^{G} \sum_{k=1}^{K} v_g v_h \frac{x_k - x_g}{\left[\left(x_k - x_g\right)^2 + \left(y_k - y_g\right)^2 + \left(z_k - z_g\right)^2\right]^{3/2}} \quad (4)$$

where G is gravitational constant; ρ_{tm} and $\rho_{m/h} = \rho_m = \rho_h$ density; g and k the gth and kth elements; G and K the total number of elements; v_g and v_k the volume of gth and kth elements; and (x_g, y_g, z_g) and (x_k, y_k, z_k) the centroid of gth and kth elements; of TM and tungsten mass mesh, respectively. Now, the total force on TM due quadrupole and hexapole is:

$$F_{total} = \sum F_m - \sum F_h \quad (5)$$

where F_m and F_h are forces on TM at a particular rotor position due to a mass and hole, respectively.

This model is used to estimate the force amplitude and uncertainty introduced by various parameters using Monte Carlo simulations. This is accomplished by turning the dimensions in table 1 into variable parameters in Ansys. We run 800 iterations by varying parameters for several rotor positions ($\omega_r t$) between $0° - 360°$. The calculated magnitude of force due to quadrupole and hexapole is summarized in table 2.

5. Conclusion

KAGRA currently uses the PCAL for detector calibration. However, the calibration uncertainty is around 3%, limited by the uncertainty in absolute laser power measurement due to the deviation in the laser power standards. Therefore, we are developing the Gravity field calibrator which can reduce this uncertainty.

As mentioned in this proceeding we have procured all of the components and are currently assembling the first prototype. In this fiscal year, we plan to finish the assembly and perform series of rotation tests to characterize the system's performance. We will also conduct a modal analysis and vibration measurement of the setup. Furthermore, we will prepare a realistic noise budget for the GCAL and evaluate the uncertainty in the calibration introduced by systematic errors using the numerical model.

The Gravity Field Calibrator developed in this study will help reduce the calibration uncertainty to a sub-percent level from the current 3%. Furthermore, the GCAL can also be used for novel gravitational experiments like measuring gravitational constant [13], testing for non-Newtonian gravity [14] and testing gravitational time delay on earth [15].

Acknowledgment

References

[1] B. P. Abbott *et al.* Observation of Gravitational Waves from a Binary Black Hole Merger. *Phys. Rev. Lett.*, 116:061102, Feb 2016.

[2] B. P. Abbott *et al.* GWTC-1: A Gravitational-Wave Transient Catalog of Compact Binary Mergers Observed by LIGO and Virgo during the First and Second Observing Runs. *Phys. Rev. X*, 9:031040, Sep 2019.

[3] R. Abbott *et al.* GWTC-2: Compact Binary Coalescences Observed by LIGO and Virgo during the First Half of the Third Observing Run. *Phys. Rev. X*, , 11:021053, Jun 2021.

[4] R. Abbott *et al.* GWTC-3: Compact Binary Coalescences Observed by LIGO andNVirgo During the Second Part of the Third Observing Run. Nov 2021.

[5] J. Aasi *et al.* Advanced LIGO. *Classical and Quantum Gravity*, 32(7):074001, April 2015.

[6] F. Acernese *et al.* Advanced Virgo: a second-generation interferometric gravitational wave detector. *Classical and Quantum Gravity*, 32(2):024001, January 2015.

[7] T. Akutsu *et al.* Overview of KAGRA: Detector design and construction history. 2021, *Prog. Theor. Exp. Phys.*, 05A101.

[8] T. Akutsu *et al.* Overview of KAGRA: Calibration, detector characterization, physical environmental monitors, and the geophysics interferometer. 2021, *Prog. Theor. Exp. Phys.*, 05A102.

[9] D. Chen, Status of KAGRA Calibration Toward O4. 2022, KIW-9, JGW-G2214100-v4 [Internal Document]

[10] D. Chen, KAGRA calibration status for O4. 2023, KIW-10, JGW-G2314929-v5 [Internal Document]

[11] Y. Inuoe *et al.* Improving the absolute accuracy of the gravitational wave detectors by combining the photon pressure and gravity field calibrators. *Phys. Rev. D.*, 98, 02200, July 2018.

[12] R. Bajpai *et al.* Estimation of Newtonian noise from the KAGRA cooling system. *Phys. Rev. D.*, 107, 042001, February 2023.

[13] A. Kawasaki *et al.* Measurement of the newtonian constant of gravitation g by precision displacement sensors. *Classical and Quantum Gravity*, 32, 075002, 2020.

[14] P. Raffai *et al.* Opportunity to test non-newtonian gravity using interferometric sensors with dynamic gravity field generators. *Phys. Rev. D.*, 84, 082002, 2011.

[15] S. Ballmer *et al.* Feasibility of measuring the shapiro time delay over meter-scale distances. *Classical and Quantum Gravity*, 27, 185018, April 2010.

PoS(ICRC2023)1550

Full Authors List: The KAGRA Collaboration

H. Abe[1], T. Akutsu[2,3], M. Ando[4,5], M. Aoumi[6], A. Araya[7], N. Aritomi[8], Y. Aso[2,9], S. Bae[10], R. Bajpai[2], K. Cannon[5], Z. Cao[11], R.-J. Chang[12], A. H.-Y. Chen[13], D. Chen[14], H. Chen[15], Y. Chen[15], A. Chiba[16], R. Chiba[17], C. Chou[18], M. Eisenmann[2], S. Fujii[17], I. Fukunaga[19], D. Haba[1], S. Haino[20], W.-B. Han[21], H. Hayakawa[6], K. Hayama[22], Y. Himemoto[23], N. Hirata[1], C. Hirose[24], S. Hoshino[24], H.-F. Hsieh[25], C. Hsiung[26], S.-C. Hsu[27,25], D. C. Y. Hui[28], K. Inayoshi[29], Y. Itoh[19,30], M. Iwaya[17], H.-B. Jin[31,32], K. Jung[33], T. Kajita[34], M. Kamiizumi[6], N. Kanda[30,19], J. Kato[16], T. Kato[17], S. Kim[28], N. Kimura[6], T. Kiyota[19], K. Kohri[35], K. Kokeyama[36], K. Komori[5,4], A. K. H. Kong[25], N. Koyama[24], J. Kume[5], S. Kuroyanagi[38,37], S. Kuwahara[5], K. Kwak[33], S. Lai[18], H. W. Lee[39], R. Lee[15], S. Lee[40], M. Leonardi[41,2], K. L. Li[12], L. C.-C. Lin[12], C-Y. Lin[42], E. T. Lin[25], G. C. Liu[26], L.-T. Ma[25], K. Maeda[16], M. Matsuyama[19], M. Meyer-Conde[19], Y. Michimura[43,5], N. Mio[44], O. Miyakawa[6], S. Miyamoto[17], S. Miyoki[6], S. Morisaki[17], Y. Moriwaki[16], M. Murakoshi[45], K. Nakamura[2], H. Nakano[46], T. Narikawa[17], L. Nguyen Quynh[47], Y. Nishino[2,48], A. Nishizawa[5], K. Obayashi[45], J. J. Oh[49], K. Oh[28], M. Ohashi[6], M. Ohkawa[24], K. Oohara[50,51], Y. Oshima[4], S. Oshino[6], M. A. Page[2], K.-C. Pan[15,25], J. Park[40], F. E. Peña Arellano[6], S. Saha[25], K. Sakai[52], T. Sako[16], R. Sato[24], S. Sato[16], Y. Sato[16], T. Sawada[6], Y. Sekiguchi[53], L. Shao[29], Y. Shikano[54,55], K. Shimode[6], H. Shinkai[56], J. Shiota[45], K. Somiya[1], T. Suzuki[24], T. Suzuki[1], H. Tagoshi[17], H. Takahashi[57], R. Takahashi[2], A. Takamori[7], K. Takatani[19], H. Takeda[58], M. Takeda[19], M. Tamaki[17], K. Tanaka[59], S. J. Tanaka[45], T. Tanaka[58], A. Taruya[60], T. Tomaru[2], K. Tomita[19], T. Tomura[6], A. Toriyama[45], A. A. Trani[5], S. Tsuchida[61], N. Uchikata[17], T. Uchiyama[6], T. Uehara[62], K. Ueno[5], T. Ushiba[6], M. H. P. M. van Putten[63], H. Wang[4], T. Washimi[2], C. Wu[15], H. Wu[15], K. Yamamoto[16], M. Yamamoto[16], T. Yamamoto[6], T. S. Yamamoto[37], S. Yamamura[17], R. Yamazaki[45], L.-C. Yang[18], Y. Yang[18], S.-W. Yeh[15], J. Yokoyama[5,4], T. Yokozawa[6], H. Yuzurihara[6], Y. Zhao[17,2], Z.-H. Zhu[11,64]

[1]Graduate School of Science, Tokyo Institute of Technology, 2-12-1 Ookayama, Meguro-ku, Tokyo 152-8551, Japan

[2]Gravitational Wave Science Project, National Astronomical Observatory of Japan, 2-21-1 Osawa, Mitaka City, Tokyo 181-8588, Japan

[3]Advanced Technology Center, National Astronomical Observatory of Japan, 2-21-1 Osawa, Mitaka City, Tokyo 181-8588, Japan

[4]Department of Physics, The University of Tokyo, 7-3-1 Hongo, Bunkyo-ku, Tokyo 113-0033, Japan

[5]Research Center for the Early Universe (RESCEU), The University of Tokyo, 7-3-1 Hongo, Bunkyo-ku, Tokyo 113-0033, Japan

[6]Institute for Cosmic Ray Research, KAGRA Observatory, The University of Tokyo, 238 Higashi-Mozumi, Kamioka-cho, Hida City, Gifu 506-1205, Japan

[7]Earthquake Research Institute, The University of Tokyo, 1-1-1 Yayoi, Bunkyo-ku, Tokyo 113-0032, Japan

[8]LIGO Hanford Observatory, Richland, WA 99352, USA

[9]The Graduate University for Advanced Studies (SOKENDAI), 2-21-1 Osawa, Mitaka City, Tokyo 181-8588, Japan

[10]Korea Institute of Science and Technology Information (KISTI), 245 Daehak-ro, Yuseong-gu, Daejeon 34141, Republic of Korea

[11]Department of Astronomy, Beijing Normal University, Xinjiekouwai Street 19, Haidian District, Beijing 100875, China

[12]Department of Physics, National Cheng Kung University, No.1, University Road, Tainan City 701, Taiwan

[13]Institute of Physics, National Yang Ming Chiao Tung University, 101 Univ. Street, Hsinchu, Taiwan

[14]Kamioka Branch, National Astronomical Observatory of Japan, 238 Higashi-Mozumi, Kamioka-cho, Hida City, Gifu 506-1205, Japan

[15]Department of Physics, National Tsing Hua University, No. 101 Section 2, Kuang-Fu Road, Hsinchu 30013, Taiwan

[16]Faculty of Science, University of Toyama, 3190 Gofuku, Toyama City, Toyama 930-8555, Japan

[17]Institute for Cosmic Ray Research, KAGRA Observatory, The University of Tokyo, 5-1-5 Kashiwa-no-Ha, Kashiwa City, Chiba 277-8582, Japan

[18]Department of Electrophysics, National Yang Ming Chiao Tung University, 101 Univ. Street, Hsinchu, Taiwan

[19]Department of Physics, Graduate School of Science, Osaka Metropolitan University, 3-3-138 Sugimoto-cho, Sumiyoshi-ku, Osaka City, Osaka 558-8585, Japan

[20]Institute of Physics, Academia Sinica, 128 Sec. 2, Academia Rd., Nankang, Taipei 11529, Taiwan

[21]Shanghai Astronomical Observatory, Chinese Academy of Sciences, 80 Nandan Road, Shanghai 200030, China

[22]Department of Applied Physics, Fukuoka University, 8-19-1 Nanakuma, Jonan, Fukuoka City, Fukuoka 814-0180, Japan

[23]College of Industrial Technology, Nihon University, 1-2-1 Izumi, Narashino City, Chiba 275-8575, Japan

[24]Faculty of Engineering, Niigata University, 8050 Ikarashi-2-no-cho, Nishi-ku, Niigata City, Niigata 950-2181, Japan

[25]Institute of Astronomy, National Tsing Hua University, No. 101 Section 2, Kuang-Fu Road, Hsinchu 30013, Taiwan

[26]Department of Physics, Tamkang University, No. 151, Yingzhuan Rd., Danshui Dist., New Taipei City 25137, Taiwan

[27]Department of Physics, University of Washington, 3910 15th Ave NE, Seattle, WA 98195, USA

[28]Department of Astronomy and Space Science, Chungnam National University, 9 Daehak-ro, Yuseong-gu, Daejeon 34134, Republic of Korea

[29]Kavli Institute for Astronomy and Astrophysics, Peking University, Yiheyuan Road 5, Haidian District, Beijing 100871, China

[30]Nambu Yoichiro Institute of Theoretical and Experimental Physics (NITEP), Osaka Metropolitan University, 3-3-138 Sugimoto-cho, Sumiyoshi-ku, Osaka City, Osaka 558-8585, Japan

[31]National Astronomical Observatories, Chinese Academic of Sciences, 20A Datun Road, Chaoyang District, Beijing, China

[32]School of Astronomy and Space Science, University of Chinese Academy of Sciences, 20A Datun Road, Chaoyang District, Beijing, China

[33]Department of Physics, Ulsan National Institute of Science and Technology (UNIST), 50 UNIST-gil, Ulju-gun, Ulsan 44919, Republic of Korea

[34]Institute for Cosmic Ray Research, The University of Tokyo, 5-1-5 Kashiwa-no-Ha, Kashiwa City, Chiba 277-8582, Japan

[35]Institute of Particle and Nuclear Studies (IPNS), High Energy Accelerator Research Organization (KEK), 1-1 Oho, Tsukuba City, Ibaraki 305-0801, Japan

[36]School of Physics and Astronomy, Cardiff University, The Parade, Cardiff, CF24 3AA, UK

[37]Department of Physics, Nagoya University, ES building, Furocho, Chikusa-ku, Nagoya, Aichi 464-8602, Japan

[38]Instituto de Fisica Teorica UAM-CSIC, Universidad Autonoma de Madrid, 28049 Madrid, Spain

[39]Department of Computer Simulation, Inje University, 197 Inje-ro, Gimhae, Gyeongsangnam-do 50834, Republic of Korea

[40]Technology Center for Astronomy and Space Science, Korea Astronomy and Space Science Institute (KASI), 776 Daedeokdae-ro, Yuseong-gu, Daejeon 34055, Republic of Korea

[41]Department of Physics, University of Trento, via Sommarive 14, Povo, 38123 TN, Italy

[42]National Center for High-performance computing, National Applied Research Laboratories, No. 7, R&D 6th Rd., Hsinchu Science Park, Hsinchu City 30076, Taiwan

[43]LIGO Laboratory , California Institute of Technology, 1200 East California Boulevard, Pasadena, CA 91125, USA

[44]Institute for Photon Science and Technology, The University of Tokyo, 2-11-16 Yayoi, Bunkyo-ku, Tokyo 113-8656, Japan

[45]Department of Physical Sciences, Aoyama Gakuin University, 5-10-1 Fuchinobe, Sagamihara City, Kanagawa 252-5258, Japan

[46]Faculty of Law, Ryukoku University, 67 Fukakusa Tsukamoto-cho, Fushimi-ku, Kyoto City, Kyoto 612-8577, Japan

[47]Department of Physics and Astronomy, University of Notre Dame, 225 Nieuwland Science Hall, Notre Dame, IN 46556, USA

[48]Department of Astronomy, The University of Tokyo, 7-3-1 Hongo, Bunkyo-ku, Tokyo 113-0033, Japan

[49]National Institute for Mathematical Sciences, 70 Yuseong-daero, 1689 Beon-gil, Yuseong-gu, Daejeon 34047, Republic of Korea

[50]Graduate School of Science and Technology, Niigata University, 8050 Ikarashi-2-no-cho, Nishi-ku, Niigata City, Niigata 950-2181, Japan

[51]Niigata Study Center, The Open University of Japan, 754 Ichibancho, Asahimachi-dori, Chuo-ku, Niigata City, Niigata 951-8122, Japan

[52]Department of Electronic Control Engineering, National Institute of Technology, Nagaoka College, 888 Nishikatakai, Nagaoka City, Niigata 940-8532, Japan

[53]Faculty of Science, Toho University, 2-2-1 Miyama, Funabashi City, Chiba 274-8510, Japan

[54]Graduate School of Science and Technology, Gunma University, 4-2 Aramaki, Maebashi, Gunma 371-8510, Japan

[55]Institute for Quantum Studies, Chapman University, 1 University Dr., Orange, CA 92866, USA

[56]Faculty of Information Science and Technology, Osaka Institute of Technology, 1-79-1 Kitayama, Hirakata City, Osaka 573-0196, Japan

[57]Research Center for Space Science, Advanced Research Laboratories, Tokyo City University, 8-15-1 Todoroki, Setagaya, Tokyo 158-0082, Japan

[58]Department of Physics, Kyoto University, Kita-Shirakawa Oiwake-cho, Sakyou-ku, Kyoto City, Kyoto 606-8502, Japan

[59]Institute for Cosmic Ray Research, Research Center for Cosmic Neutrinos, The University of Tokyo, 5-1-5 Kashiwa-no-Ha, Kashiwa City, Chiba 277-8582, Japan

[60]Yukawa Institute for Theoretical Physics (YITP), Kyoto University, Kita-Shirakawa Oiwake-cho, Sakyou-ku, Kyoto City, Kyoto 606-8502, Japan

[61]National Institute of Technology, Fukui College, Geshi-cho, Sabae-shi, Fukui 916-8507, Japan

[62]Department of Communications Engineering, National Defense Academy of Japan, 1-10-20 Hashirimizu, Yokosuka City, Kanagawa 239-8686, Japan

[63]Department of Physics and Astronomy, Sejong University, 209 Neungdong-ro, Gwangjin-gu, Seoul 143-747, Republic of Korea

[64]School of Physics and Technology, Wuhan University, Bayi Road 299, Wuchang District, Wuhan, Hubei, 430072, China